Cell-specific effects of RB or RB/p107 loss on retinal development implicate an intrinsically death-resistant cell-of-origin in retinoblastoma

Danian Chen,[1] Izhar Livne-bar,[1] Jackie L. Vanderluit,[2] Ruth S. Slack,[2] Mahima Agochiya,[1] and Rod Bremner[1,*]

[1]Toronto Western Research Institute, University Health Network, Vision Science Research Program, Department of Ophthalmology and Visual Sciences and Department of Laboratory Medicine and Pathobiology, University of Toronto, 399 Bathurst Street, Toronto, Ontario, Canada, M5T 2S8
[2]Ottawa Health Research Institute, University of Ottawa, 451 Smyth Road, Ottawa, Ontario, Canada K1H 8M5
*Correspondence: rbremner@uhnres.utoronto.ca

Summary

Retinogenesis involves expansion of pluripotent progenitors, specification of postmitotic precursors, and terminal differentiation. *Rb* or *Rb/p107* loss causes retinoblastoma in humans or mice, respectively. One model suggests that *Rb*- or *Rb/p107*-deficient retinal precursors have infinite proliferative capacity but are death-prone and must acquire an antiapoptotic mutation. Indeed, we show that *Rb/p107* loss does not affect progenitor proliferation or precursor specification, but perturbs cell cycle exit in all seven retinal precursors. However, three precursors survive *Rb/p107*-loss and stop proliferating following terminal differentiation. Tumors arise from precursors that escape this delayed growth arrest. Thus, retinoblastoma arises from a precursor that has extended, not infinite, proliferative capacity, and is intrinsically death-resistant, not death-prone. We suggest that additional lesions common in retinoblastoma overcome growth arrest, not apoptosis.

Introduction

The mature retina consists of three nuclear layers and seven major cell types (Figure 1A). Cell bodies of photoreceptors (rods and cones) reside in the outer nuclear layer (ONL), while those of horizontal, bipolar, and amacrine interneurons and Müller glia lie in the inner nuclear layer (INL) (Figure 1A). The innermost layer is the ganglion cell layer (GCL), which consists of a 1:1 mix of ganglion and amacrine neurons. Mature retinal cells derive from dividing "progenitors" in the neuroblastic layer (NBL) (Figure 1A). Their cell bodies oscillate within the NBL during the cell cycle. M phase progenitors are on the outer edge of the NBL (Figure 1A), and S phase progenitors in the inner half of this layer. After mitosis, G1 cells migrate inward to the inner NBL, and after S phase, G2 cells migrate back outward (Figure 1A). Daughters can remain as dividing progenitors or exit the cell cycle to generate postmitotic "precursors." For clarity, we will use the term progenitor to refer to pluripotent dividing cells. In contrast, we use the term precursor to define postmitotic cells that have not yet terminally differentiated. Precursors eventually differentiate into one of the seven major retinal cell types.

In mice, ganglion, horizontal, cone, and amacrine precursors are born (exit the cell cycle) embryonically, bipolar and Müller cells are born postnatally (Figure 1B), and rods are born pre- and postnatally (Figure 1B). Division ends by P8 in the central retina and P10 in the far periphery (Young, 1985). The fate of postmitotic precursors is determined by transcription factors, many of which are basic-helix-loop-helix (bHLH) and homeodomain proteins. Of particular relevance here are the bHLH factors Math3 and NeuroD, required to specify amacrine neurons (Inoue et al., 2002), and Hes5, which drives Müller cell formation (Hojo et al., 2000), as well as the homeodomain proteins Prox1, necessary for horizontal cell formation (Dyer et al., 2003), Chx10, expressed in all progenitors and required for bipolar cell genesis (Burmeister et al., 1996), Crx, expressed in rod and cone precursors and required for their terminal differentiation (Chen et al., 1997; Freund et al., 1997; Furukawa et al., 1997), and Brn3b, required for ganglion cell specification (Erkman et al., 1996; Gan et al., 1996).

RB can influence cell division, survival, and differentiation, but its role in the retina is unclear. RB could target the rate and/or extent of progenitor proliferation, the specification of

SIGNIFICANCE

The "cell-of-origin" is a critical but poorly understood aspect of cancer. Elucidating its properties would facilitate development of novel preventative and early intervention therapies. Indirect evidence suggests that retinal cells typically die in response to *Rb* loss; thus, tumors must arise from clones that acquire resistance to apoptosis. Using an inheritable mouse model of retinoblastoma induced by *Rb* loss, we find that the cell-of-origin may be naturally death-resistant. Tumors arise from clones that escape terminal differentiation-associated growth-arrest, not death. Thus, tumors exploit a natural property of the cell-of-origin that is a hallmark of cancer cells, which helps explain why retinoblastoma arises in few steps, and reveals that enhanced survival is not always an acquired event in tumorigenesis.

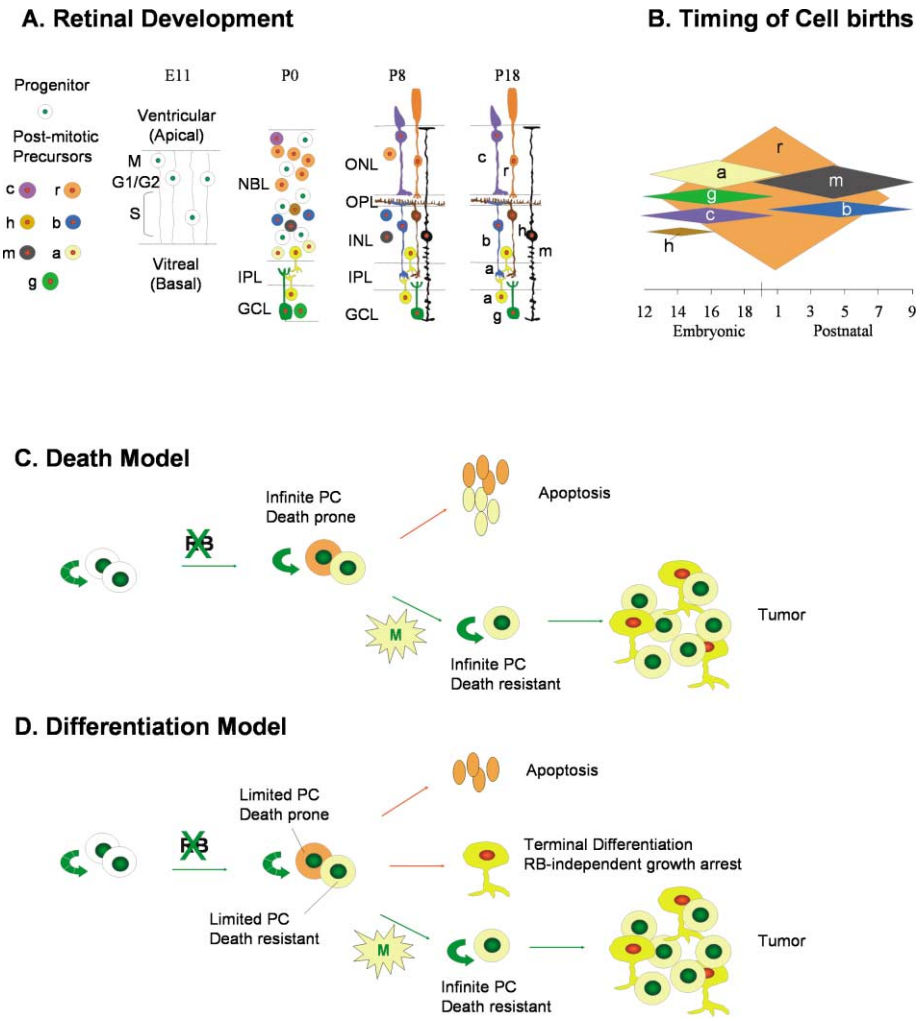

Figure 1. Models of retinoblastoma

A: Retinal development. At E11, the retina consists of a neuroblastic layer (NBL) made up of dividing progenitors (white circle, green nuclei). See text for explanation of position of oscillating cell bodies and relation to cell cycle phase. At P0, the NBL contains a mix of progenitors and postmitotic precursors (colored circles, red nuclei) and is separated from the differentiated ganglion cell layer (GCL) by the inner plexiform layer (IPL). By P8, there are no progenitors, fewer precursors, and more differentiated rods (r), cones (c), horizontal (h), bipolar (b), Müller (m), amacrine (a), and ganglion (g) cells. Retinal development is essentially complete by P18.

B: Timing of cell births. The period when each precursor is born (exits the cell cycle) is diagrammed.

C: Death model. Progenitors with finite proliferative capacity (PC, broken green curved arrow) normally differentiate into postmitotic precursors which differentiate into seven retinal cell types. RB loss does not block precursor specification, but generates cells with infinite PC (green curved arrow). Ectopically dividing precursors are deleted by apoptosis. Tumors only arise when another mutation (M) renders precursors death-resistant.

D: Differentiation model. Here, precursors only have limited PC (broken green curved arrow). Some precursors (mouse c, r, b, g—see text) are deleted by apoptosis. However, others (h, a, m—see text) tolerate ectopic division, and eventually exit the cell cycle by RB-independent means linked to terminal differentiation. Tumors only arise when another mutation (M) generates cells with the ability to divide indefinitely.

precursors, cell cycle exit in one or more precursors, and/or terminal differentiation. RB is detectable in the embryonic GCL, but not NBL, suggesting that it may regulate cell birth and/or differentiation (Gallie et al., 1999; Jiang et al., 1997). Indeed, ectopically dividing cells can be detected in the GCL of *Rb*$^{-/-}$ mice at E13 (Saavedra et al., 2002). These embryos perish soon after E13, but explant studies revealed that the *Rb*$^{-/-}$ retina produces more cells than the wild-type retina (Zhang et al., 2004). This result supports the idea that *Rb* loss might result in ectopic precursor division, but does not rule out the alternative that progenitor cells cycle faster or for an extended period. Indeed, the same study detected RB in dividing progenitors as well as postmitotic cells in the postnatal retina (Zhang et al., 2004). Thus, a comprehensive analysis of the effects of *Rb* loss on the cell cycle in progenitors and precursors is required.

Human retinoblastoma tumors contain several recurrent genetic changes in addition to *Rb* inactivation (Chen et al., 2001, 2002). For example, 1q31 and 6p22 gains are present in at least 50% of tumors. One hypothesis suggests that *Rb* loss confers infinite proliferative capacity on retinal precursors, but ectopically dividing cells die unless they accumulate an antiapoptotic mutation prior to their demise (Figure 1C) (Gallie et al., 1999). Three strands of evidence indirectly support the idea that post-*Rb* lesions may overcome apoptosis. First, SV40 large T antigen (Tag), which inactivates both RB and the proapoptotic protein p53, transforms photoreceptor precursors (Al-Ubaidi et al., 1992a), but human papilloma virus protein E7, which targets RB but not p53, induces apoptosis in these cells in wild-type mice and tumors in p53$^{-/-}$ mice (Howes et al., 1994). Thus, bypassing a death pathway may be a prerequisite for retinal cell transformation. Second, the death of *Rb*$^{-/-}$ embryos is linked to apoptosis in several tissues (Clarke et al., 1992; Jacks et al., 1992; Lee et al., 1992). However, in chimeric mice, *Rb*$^{-/-}$ embryonic stem (ES) cells contribute to most tissues as efficiently as wild-type cells, demonstrating that cell death in the *Rb*$^{-/-}$ embryo is indirect. Indeed, most apoptosis in these embryos is secondary to a placental defect (Wu et al., 2003). Notably, however, *Rb*$^{-/-}$ cells contribute poorly to chimeric retinas, supporting the idea that apoptosis is the default response of *Rb*-deficient retinal cells. Finally, although Rb$^{+/-}$ mice develop pituitary tumors rather than retinoblastoma, chimeras generated using *Rb*$^{-/-}$;p107$^{-/-}$ ES cells develop sporadic retinoblastoma amid a mass of dying cells (Robanus-Maandag et al., 1998), arguing, again, that the retinoblastoma cell-of-origin faces an early battle with death (Figure 1C). In this model, tumor cells must acquire a mutation that overcomes the tendency for ectopically dividing cells to die.

Several issues should be considered in assessing the above death model. First, although RB regulates retinal proliferation (Zhang et al., 2004), it is unclear whether it modulates the rate of division in progenitors and/or the timing of cell cycle exit during the transition to postmitotic precursors. Second, *p53* is intact in human retinoblastoma (Gallie et al., 1999); thus, viral oncoprotein expression in photoreceptor precursors may not mimic the origins of the human disease. Third, while chimeric studies suggest some cell autonomous death of $Rb^{-/-}$ or $Rb^{-/-}$;$p107^{-/-}$ retinal cells, it is unclear whether all or only a subset of cell types are affected. Indeed, inactivation of *Rb* and *p107* in the developing cerebellum induces apoptosis in granule, basket, and stellate neurons, but Purkinje neurons and Bergmann glia survive (Marino et al., 2003). Fourth, it is also unclear whether precursors could divide indefinitely if they did survive. Thus, direct evidence for the death model (Figure 1C) is lacking.

To study the role of RB and p107 in retinogenesis and retinoblastoma, we exploited conditional inactivation of *Rb* in the retina of $p107^{-/-}$ mice. *Rb/p107* inactivation did not affect progenitor division, or precursor specification, but resulted in ectopic proliferation of all retinal precursors, implicating these cells, rather than progenitors, as the source of retinoblastoma. In tumor-prone double knockout (DKO) retina, four precursor types died prior to maturation, but three INL precursors survived and generated terminally differentiated horizontal, amacrine, and Müller cells. Critically, these cells stopped dividing even in the absence of RB/p107. Sporadic tumors arose that escaped growth arrest and expressed transcription factor determinants of the surviving, intrinsically death-resistant precursors. These data support an alternative retinoblastoma model in which death-resistant precursors with extended but not infinite proliferative capacity must overcome differentiation-induced growth arrest rather than apoptosis (Figure 1D). The post-*Rb* genetic defects common in human retinoblastoma may facilitate this process. The idea of a naturally death-resistant cell-of-origin may partially explain why retinoblastoma arises in fewer genetic steps than adult tumors and suggests that tumor resistance to apoptosis is not always acquired through mutation.

Results

A subset of RBKO or DKO retinal cells survive and differentiate

To study the cell-specific effects of *Rb* or *Rb/p107* loss in the retina, we crossed floxed *Rb* mice (Marino et al., 2000; Vooijs et al., 2002) with a strain carrying a Cre recombinase transgene under the control of the *Pax6* α-enhancer (α-*Cre*), which is active in peripheral retinal progenitors at embryonic day ten (E10, Figure 2A) (Marquardt et al., 2001). *Rb* deletion in progenitors mimics human retinoblastoma, where, by definition, lesions must occur in dividing cells. *Rb* inactivation in the peripheral retina of $Rb^{loxp/loxp}$; α-*Cre* and $Rb^{loxp/loxp}$;$p107^{-/-}$;α-*Cre* animals was confirmed by PCR analysis and immunofluorescence (Figures 2B and 2C). Hereafter, the wild-type, $Rb^{-/-}$, and $Rb^{-/-}p107^{-/-}$ genotypes are referred to as WT, RBKO, and DKO, respectively.

In the mature RBKO retina, ganglion (Brn3b) and bipolar cells (PKC, Vsx1) were much reduced, and there were fewer rods (rhodopsin, rod arrestin) (Figure 2D, Supplemental Figures S1A–S1C at http://www.cancercell.org/cgi/content/full/5/6/539/DC1). In contrast, many cone (cone arrestin), amacrine (Pax6, syntaxin), horizontal (Calbindin), and Müller (CRALBP) cells were detected (Figure 2E). Quantification showed that the number of cones and amacrine and horizontal neurons in the mature RBKO or WT retinas were similar (Supplemental Figures S1D–S1F). Cones had stunted segments, likely an indirect consequence of fewer rods (Usukura et al., 1994). In the DKO retina, ganglion and bipolar cells were also absent, and in addition, all rods and cones were missing (Figure 2D, Supplemental Figures S1A–S1D). Remarkably, amacrine, horizontal, and Müller glia were preserved (Figure 2E), and quantification revealed WT numbers of $Pax6^+$ amacrine and $Calbindin^+$ horizontal neurons in the mature DKO retina (Supplemental Figures S1E and S1F).

The absence of specific neurons in RBKO or DKO retina was reflected in the structure of the plexiform layers. In the RBKO retina, fewer rod and bipolar synapses thinned the outer plexiform layer (OPL) (Figure 2C). In the DKO retina, which lacked rods, cones, and bipolar cells, the OPL was absent (Figure 2C). In accordance with the loss of synaptic contacts, horizontal cell processes were disorganized in the RBKO retina and virtually absent in the DKO retina (Figure 2E). The dramatic structural difference in the OPL accurately marked the transition between WT central and KO peripheral retina, as it was clearly visible with a nuclear DAPI stain, and precisely correlated with the loss of RB expression (Figure 2C).

In contrast to the OPL, a distinct inner plexiform layer (IPL) was detected in the mature RBKO or DKO retina (Figures 2C–2E), but consisted entirely of amacrine processes, since both bipolar and ganglion cells were absent (Figures 2D and 2E). Calretinin staining, which marks a subset of amacrine and ganglion cells, highlighted three strata in the WT IPL, but only one in the RBKO or DKO IPL (arrows, Figure 2E).

Precursors of missing cells are specified in the absence of RB/p107

Cell loss in mutant retinas could indicate a role for RB in differentiation or survival. To determine whether RB affects cell type specification, we surveyed a variety of fate determinants and/or specific precursor markers. Brn3b is expressed in precursor and mature ganglion cells and is essential for their development (Erkman et al., 1996; Gan et al., 1996). $Brn3b^+$ cells were absent in mature RBKO or DKO retina (Figure 2D), but many positive cells were found at E17, and their numbers diminished severely by P0 (Figure 3). Crx is critical for the proper terminal differentiation of photoreceptors, but is also present in rod/cone precursors (Chen et al., 1997; Furukawa et al., 1997). Despite the absence of rods in the mature DKO retina, Crx^+ precursors were detected in the presumptive ONL at E17 and P0, but had reduced significantly by P8 (Figure 3). Crx is also present in bipolar cells (Bibb et al., 2001), and consistent with the later birth of bipolar cells, Crx staining was observed in the presumptive INL at P8 (Figure 3); the bipolar identity of these cells was confirmed by staining for Chx10, which is essential for bipolar differentiation (Figure 3) (Burmeister et al., 1996). The nuclear receptor Trβ2 specifies a major subset of cones (green cones) (Ng et al., 2001). Cones were missing in the mature DKO retina (Figure 2D), but many $Tr\beta2^+$ precursors were detected in the presumptive ONL at E17 (Figure 3). Thus, the absence of rod, cone, bipolar, and ganglion cells in the mature DKO retina was not due to a lack of precursor specification.

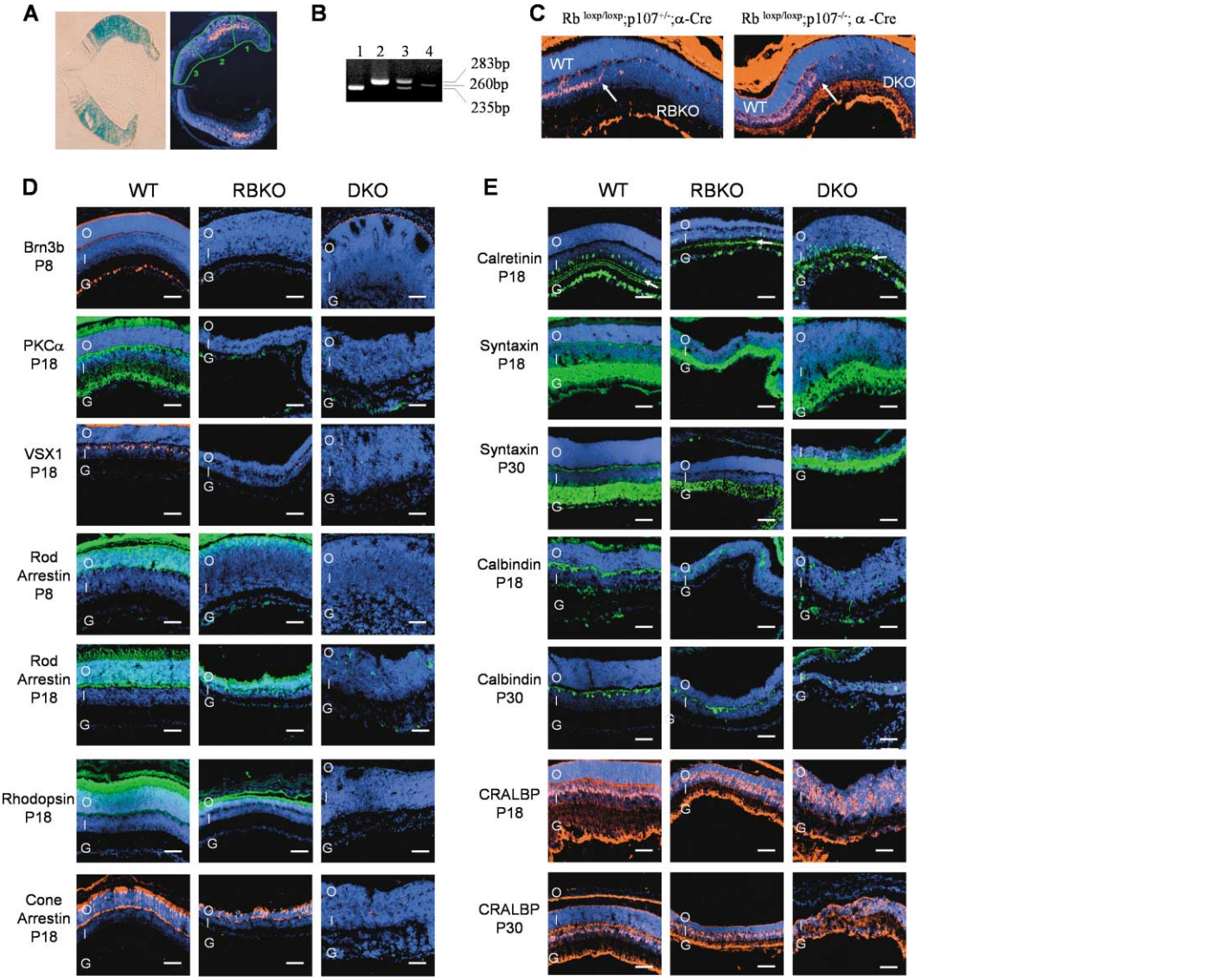

Figure 2. A subset of RBKO or DKO INL cells survive and differentiate

A: Left panel: X-Gal stained *Rosa26R;α-Cre* E16 retina showing Cre activity in peripheral but not central retina. Right panel: Diagram of bins used to quantify cell numbers; a DAPI (blue) and TUNEL (red) stained P8 $Rb^{loxP/loxP};p107^{-/-};$*α-Cre* retina stained is shown.

B: Genotyping of tail DNA from WT (lane 1), $Rb^{loxP/loxP}$ (lane 2), and $Rb^{loxP/+}$ (lane 3) mice, and peripheral retina DNA from $Rb^{loxP/loxP}$*;α-Cre* mice (lane 4). 235 bp, 260 bp, and 283 bp products represent WT (primers Rb19E and Rb18), recombined (primers Rb212 and Rb18) and floxed Rb alleles (primers Rb19E and Rb18), respectively.

C: Overlay of DAPI (blue) and anti-RB immunofluorescence (red) on horizontal sections from $Rb^{loxP/loxP};p107^{+/-};$*α-Cre* and $Rb^{loxP/loxP};p107^{-/-};$*α-Cre* retinas. Strong RB expression is visible in Müller glia, with very low levels in other cells. Arrows indicate boundary between central WT and peripheral RBKO or DKO regions.

D and E: Mature cell types in RBKO or DKO retina. Missing cells in the DKO retina are shown in **D**, surviving differentiated cells in **E**. Horizontal retinal sections from mice of the indicated ages and genotypes were stained for nuclei (DAPI, blue) and markers that detect ganglion cells (Brn3b, red), rod bipolar (PKCα, green), and cone bipolar (Vsx1, red) cells, rods and cones (rod arrestin, green), rods (rhodospin, green), cones (cone arrestin, red), amacrine cells (calretinin, green, arrows indicate reduction of three synaptic strata in WT to one in RBKO or DKO), amacrine and horizontal cells (syntaxin, green), horizontal and a subset of amacrine cells (calbindin, green), and Müller glia (CRALBP, red). O, ONL. I, INL. G, GCL. Scale bar = 50 μm.

Death of RB/107-deficient ganglion but not amacrine precursors

The above data suggest that missing cells may have died prior to terminal differentiation. Indeed, the reduced thickness of the RBKO or DKO P30 retina (Figure 2E) was consistent with cell loss. TUNEL analysis revealed elevated apoptosis at P0, P8, and P18 in the RBKO or DKO retina (Figure 4A). Cell death was higher in the DKO (Figure 4B), consistent with the fact that DKO mice lack ganglion, bipolar cells, rods, and cones, whereas RBKO mice have many rods and all cones (Figure 2D). TUNEL peaked at P8 (Figure 4A) corresponding to the disappearance of Crx^+ rods and $Crx^+/Chx10^+$ bipolar cells from the DKO retina between P0 and P8 (Figure 3).

To examine cell death more closely, we compared amacrine and ganglion cells, which are born at similar times (Figure 1B), but have opposite fates in the absence of RB (Figures 2D and

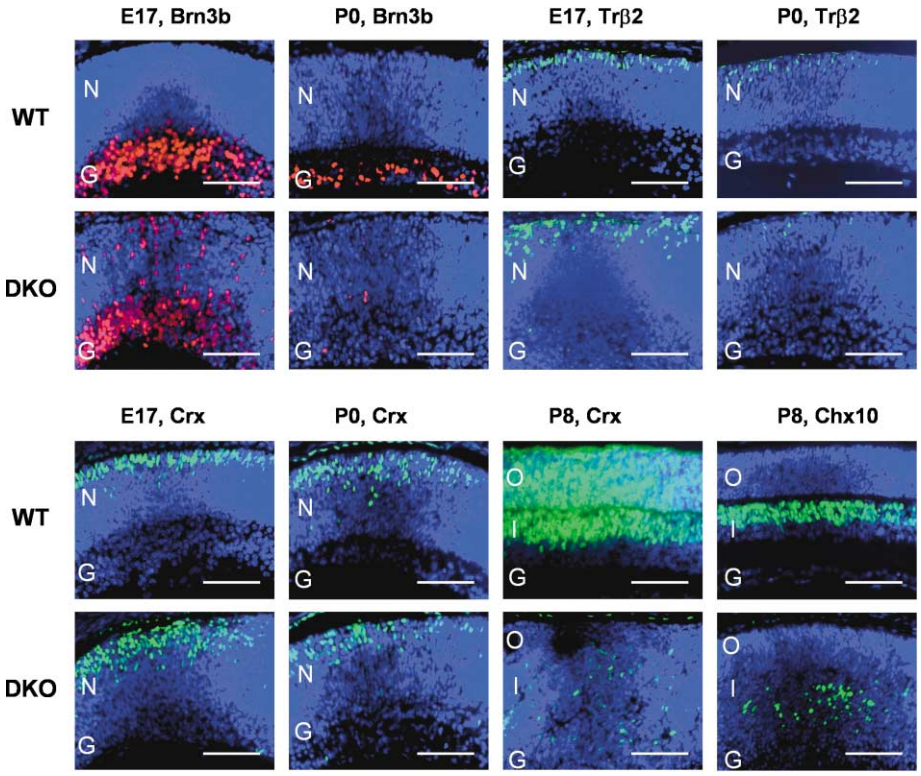

Figure 3. Deleted DKO cell types are specified normally

Retinas of the indicated genotype and ages were stained for DAPI (blue) and transcription factor determinants/markers (red or green) of ganglion (Brn3b), cone (Trβ2), photoreceptor (Crx), or bipolar (Chx10, Crx) precursors. Figure 1B shows timing of specification of each cell type. N, NBL. O, ONL. I, INL. G, GCL. Scale bar = 50 μm.

2E). We attempted double labeling by TUNEL plus cell-specific markers, but DNA fragmentation is an end-stage apoptotic event, thus markers are often degraded (c.f. Rakic and Zecevic, 2000). Activation of caspase 3, an apoptotic effector protease, occurs earlier in the death cascade (Watanabe et al., 2002), and this marker was identified in DKO cells (Figure 4C). Brn3b specifically marks 70% of ganglion cells (Xiang et al., 1993), while Pax6 stains both amacrine cells and over 90% of Brn3b$^+$ ganglion cells (data not shown). Thus, we reasoned that if both amacrine and ganglion cells were dying in the DKO retina, more active caspase 3 positive (AC3$^+$) cells would express Pax6 (amacrine + ganglion) than Brn3b (ganglion only). Instead, the proportion of AC3$^+$ cells in the inner third of the DKO E17 retina that were Brn3b$^+$ or Pax6$^+$ was identical (Figures 4C and 4D). Some cells stained for AC3 but not Brn3b or Pax6; these cells could be either Brn3b$^-$ or Pax6$^-$ ganglion cells, or late stage Brn3b$^+$ or Pax6$^+$ apoptotic cells that had undergone significant proteolysis. These data, coupled with the disappearance of Brn3b$^+$ DKO ganglion precursors between E17 and P0, the presence of many Pax6$^+$ DKO cells at P0 and P8 (Figures 3 and 5F and Supplemental Figures S1A and S1F), and the many mature DKO amacrine cells at P30 (Figure 2E), suggest that ganglion precursors are deleted, but many amacrine precursors survive and terminally differentiate.

It was difficult to confirm directly that photoreceptor or bipolar precursors also die by apoptosis, because the AC3 antibody and Crx, Trβ2, or Chx10 antibodies were from the same species and other AC3 antibodies we tried did not work well. However, cones and ganglion cells are born at similar times (Figure 1B), and the disappearance of cones closely paralleled that of ganglion cells (Figure 3). Rod and bipolar precursors also disappeared soon after specification; rod births peak at P0 (Figure 1B) and Crx$^+$ cells declined between P0 and P8 in the outer retina (Figure 3). Also, rods account for 70% of retinal cells, and the peak of TUNEL staining around P8 (Figures 4A and 4B) correlated with their demise. Bipolar neurons account for 10% of retinal cells, and the low level of Chx10$^+$ cells at P8 (Figure 3) correlated with the peak of bipolar cell births at P4 (Figure 1B). In the chimeric retina, the product of an IRBP-p53 transgene present in DKO cells was only detected at early stages of development (Robanus-Maandag et al., 1998). The IRBP promoter drives expression in newly born and mature photoreceptors, which supports our conclusion that these cells are deleted prior to maturation. Altogether, these data suggest that DKO ganglion, rod, cone, and bipolar cells are specified, but then die by apoptosis prior to maturation.

Ectopic division of all precursors in the RBKO or DKO retina

We next assessed whether RB loss caused ectopic division in the retina. These analyses were important to test the idea that RB-deficient retinal precursors have infinite proliferative capacity (Figure 1C). Also, if precursor cell death follows ectopic proliferation, a facile explanation for the survival of a subset of retinal precursors would be that these cells do not require RB to exit the cell cycle.

Mice of various ages were labeled with BrdU for two hours prior to sacrifice, and anti-BrdU immunostaining used to locate S phase cells (Figure 5A). At P0, the number of S phase cells was similar in all genotypes (Figure 5B), but ectopic S phase cells could be observed at the outer edge of the RBKO or DKO retina, the location of maturing photoreceptors, and in the inner retina, where amacrine and ganglion cells reside (Figure 5A). Quantification of ectopic S phase cells in the GCL revealed

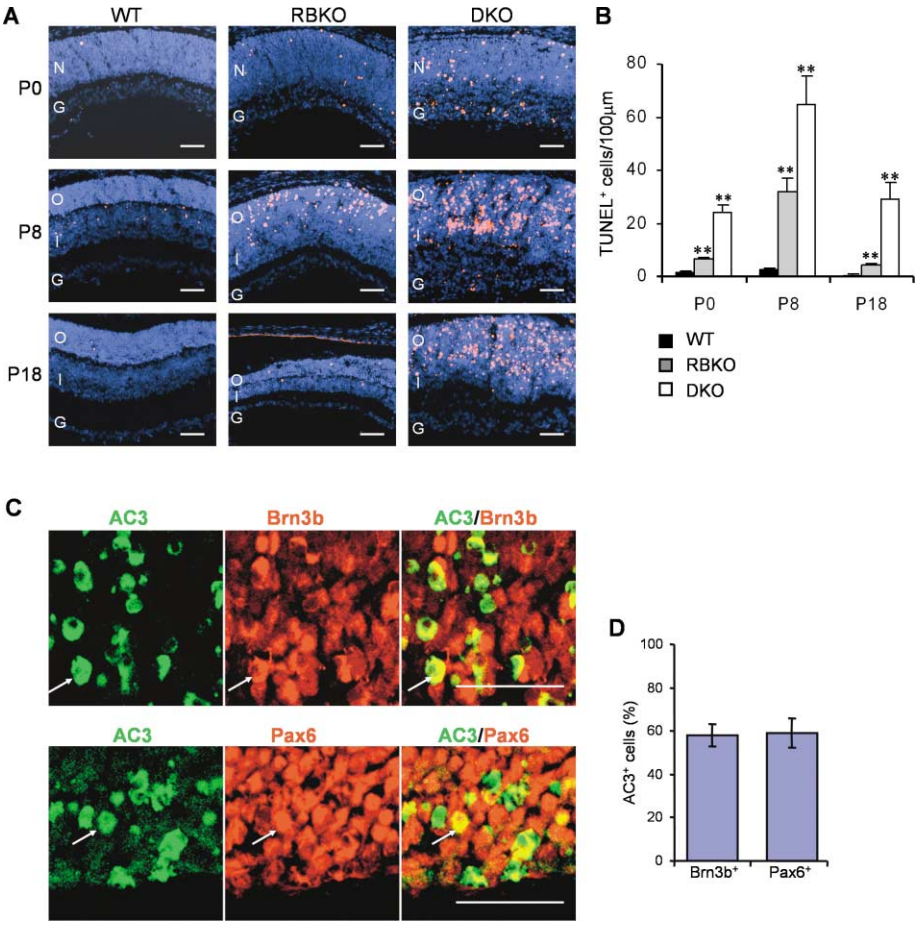

Figure 4. Apoptosis in the RBKO and DKO retina is cell-specific

A: Horizontal sections of the indicated genotypes and ages were stained for nuclei (DAPI, blue) and apoptosis (TUNEL, red). N, NBL. O, ONL. I, INL. G, GCL.

B: Quantification of total TUNEL$^+$ cells.

C and D: Death of ganglion but not amacrine precursors. **C:** E17 DKO retina was stained with antibodies against AC3 (green) to mark apoptotic cells and Brn3b (top panel, red) or Pax6 (bottom panel, red) to mark ganglion cells alone or ganglion plus amacrine cells, respectively. Arrows indicate examples of double-labeled cells. Quantification (**D**) of confocal images revealed that a similar proportion of AC3$^+$ cells in the inner third of the retina were Brn3b$^+$ or Pax6$^+$. Error bars represent SD and asterisks indicate significant difference between normal and RB or DKO retina (*, $p < 0.05$, **, $p < 0.01$, Student's t test). Scale bar in **A** and **C** is 50 μm.

significant increases both in the RBKO and DKO retina (Figure 5C). At P8, there were many BrdU$^+$ cells in the RBKO or DKO retina, which contrasted markedly with the WT retina, in which division had virtually ceased (Figure 5A). The total number of ectopic BrdU$^+$ cells in the DKO retina was 2.5- and 4-fold above the RBKO retina at P8 and P18, respectively (Figure 5B). Surprisingly, ectopic division ceased in the DKO retina by P30 (Figure 5A), contradicting the idea that RB-deficient precursors have infinite proliferative capacity (Figure 1C).

To determine whether all or only the subset of DKO retinal cells underwent ectopic division, we performed a series of double labeling experiments. As described earlier, a similar fraction of AC3$^+$ apoptotic cells in the inner E17 retina were Brn3b$^+$ or Pax6$^+$ (Figure 4D). In contrast to these apoptosis assays, the fraction of dividing Pax6$^+$ amacrine plus ganglion cells at E17 greatly exceeded the fraction of dividing Brn3b$^+$ ganglion cells (Figures 5D and 5E), suggesting that both ganglion and amacrine precursors were dividing ectopically. There were no dividing Brn3b$^+$ or Pax6$^+$ cells in the inner WT retina at E17 (data not shown). Moreover, at P0 and P8, when there were few remaining ganglion cells (Figures 2D and 3), there were still many Pax6$^+$/BrdU$^+$ cells in the RBKO or DKO inner retina (Figure 5F and data not shown). An additional assay was performed to confirm that amacrine precursors divide ectopically. Amacrine cell birth is virtually complete by P1, and the remaining progenitors give rise to rod, Müller, and bipolar cells (Figure 1B). We injected mice daily with BrdU from P1–P8. If amacrine precursors had exited the cell cycle, only labeled rod, Müller, and bipolar cells would have been detected in mutant retina. Instead, many BrdU$^+$ amacrine cells were observed in the inner RBKO or DKO retina (Figure 5G and data not shown).

We also analyzed whether other DKO retinal precursors divide ectopically. Math3 is expressed in bipolar and amacrine precursors (Inoue et al., 2002), and Hes5 is expressed in Müller precursors (Hojo et al., 2000). In situ analysis coupled with BrdU labeling showed that cells expressing Math3 and Hes5 were dividing in DKO but not WT retina (Supplemental Figure S2). Prox1 is required for horizontal cell differentiation and is also expressed in a subset of amacrine neurons (Dyer et al., 2003). Horizontal cells only constitute 1% of the retina, and occasional ectopically dividing Prox1$^+$ cells were observed in the DKO but not WT outer retina at P8 (Supplemental Figure S2). Larger numbers were seen in the inner retina corresponding to a Prox1$^+$ subset of amacrine precursors (Dyer et al., 2003). Finally, dividing Crx$^+$ and Chx10$^+$ photoreceptor and bipolar precursors were also detected in the DKO, but not WT P8 retina (Supplemental Figure S2).

Altogether, these data show that all precursors divide ectopically, including those that survive RB or RB/p107 loss.

RB or RB/p107 loss does not affect progenitor cell division

The above data show that RB is required for the correct timing of cell cycle exit in specified precursors, but do not reveal

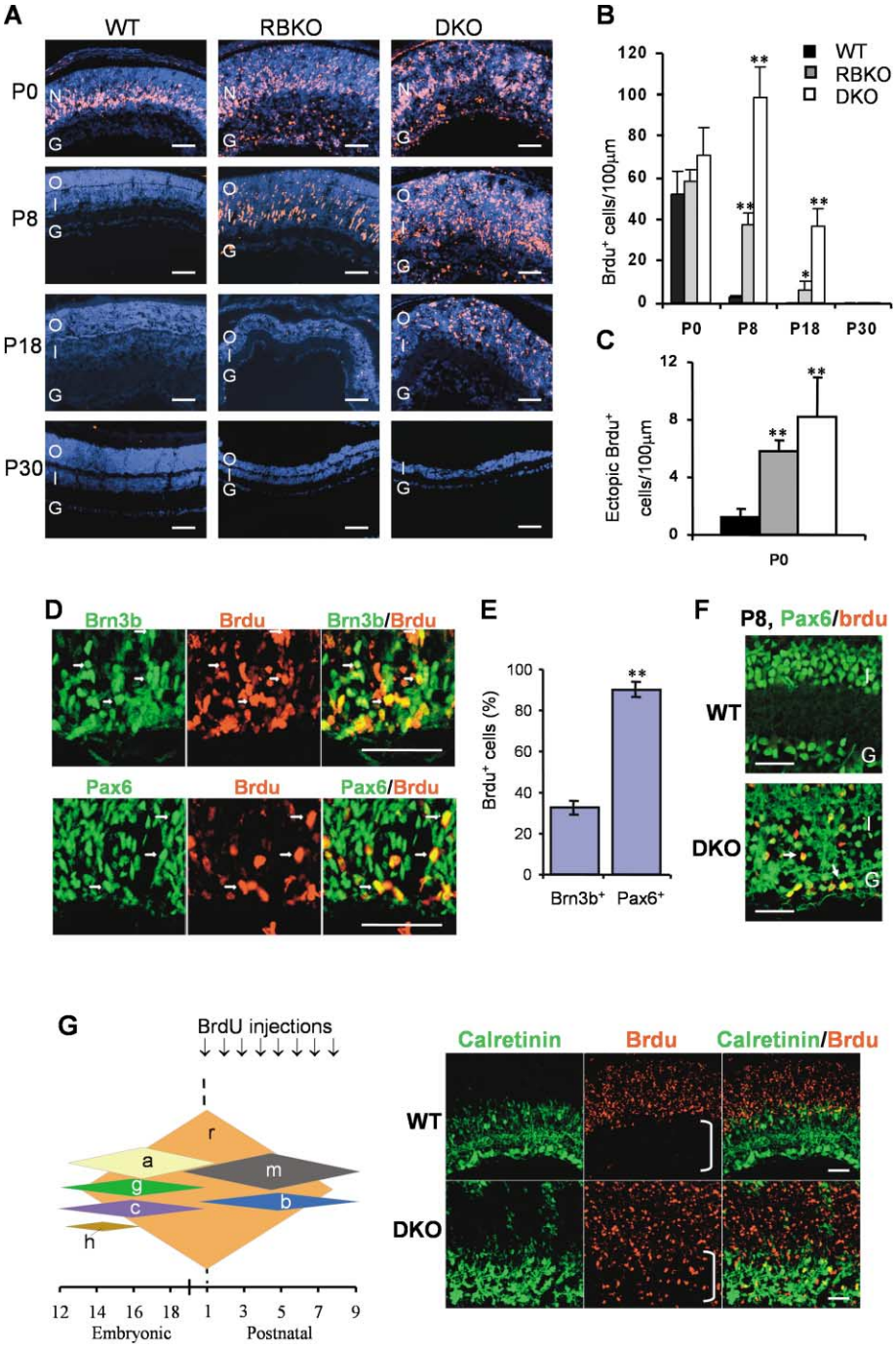

Figure 5. Ectopic division of precursors in RBKO and DKO retinas

A: Horizontal sections of the indicated genotypes and ages were stained for nuclei (DAPI, blue) and S phase (anti-BrdU, red). N, NBL. O, ONL. I, INL. G, GCL.

B: Quantification of all BrdU+ cells.

C: Quantification of ectopic BrdU cells in GCL at P0.

D and E: Ectopic division of ganglion and amacrine cells. **D:** E17 DKO retina was stained with antibodies against BrdU (red) and Brn3b (top panel, green) or Pax6 (bottom panel, green) to mark ganglion cells alone or ganglion plus amacrine cells, respectively. Arrows indicate examples of double-labeled cells. Quantification (**E**) of confocal images revealed that a greater proportion of BrdU$^+$ cells in the inner third of the retina were Pax6$^+$ than Brn3b$^+$. Contrast this data with apoptosis of these cells (Figure 4D).

F: Dividing Pax6$^+$ DKO amacrine cells at P8. P8 retina of indicated genotype was stained for Pax6 (green) and BrdU (red). Arrows indicate examples of double-labeled cells.

G: BrdU labeling of ectopically dividing amacrine precursors. Most amacrine cells (a) are born prior to P1 (schematic diagram, see Figure 1 for abbreviations). BrdU was injected each day from P1–P8 (arrows). P8 retinal sections were stained for Calretinin (green) and BrdU (red). Brackets indicate position of amacrine neurons, which are only BrdU$^+$ in the DKO retina. Müller, bipolar, and rods are born postnatally, so they are BrdU$^+$ in WT and DKO retina. Error bars as in Figure 4. Scale bar in **A**, **D**, **F** and **G** is 50 μm.

whether RB and/or p107 also modulate the cell cycle in dividing progenitors. RB loss could alter progenitor division in two ways. First, it might prevent progenitors from differentiating into precursors, biasing cells to adopt later fates. However, as shown above, there were many early born ganglion, amacrine, and photoreceptor precursors in the embryonic DKO retina (Figure 3) suggesting that, although RB loss uncouples cell cycle arrest in differentiating precursors, it does not impair differentiation of progenitors into precursors.

Second, RB loss might increase progenitor proliferation without altering when they differentiate into precursors. Antibodies to phosphohistone H3, an M phase marker, stained normal mitotic progenitors on the outer edge of the retina together with several ectopic mitoses in RBKO or DKO retina (Figure 6A, arrow). As with S phase cells, mitotic cells were observed both in unusual positions and times (Figure 6A), and these effects were more prominent and persistent in the DKO retina (Figures 6A and 6B). However, despite the presence of ectopic dividing cells in the inner layers, the number of normal progenitor mitoses on the outer edge of the retina was not significantly different in WT, RBKO, or DKO E17 or P0 retina (Figure 6C). In addition, we counted the number of Chx10$^+$ cells at E17. At this stage,

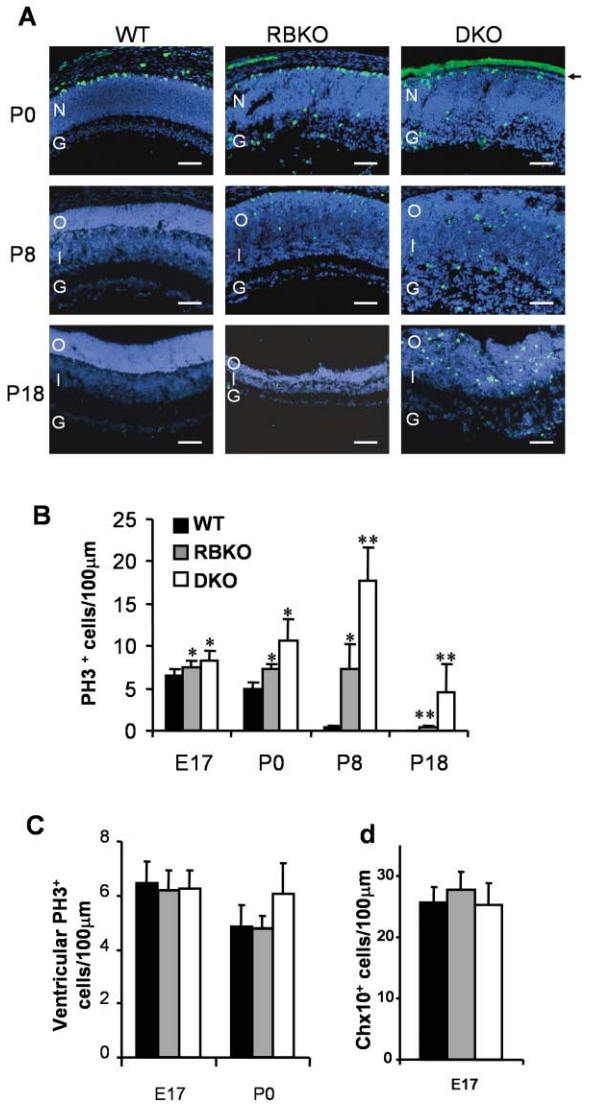

Figure 6. Normal progenitor proliferation in RBKO or DKO retina

A: Horizontal sections of the indicated genotypes and ages were stained for nuclei (DAPI, blue) and mitosis (phosphohistone H3, green). Arrow indicates the position of normal mitoses on the outer edge of the retina. N, NBL. O, ONL. I, INL. G, GCL.

B: Quantification of total PH3$^+$ cells in RBKO or DKO retina.

C: Quantification of ventricular (i.e., progenitor) PH3$^+$ cells.

D: Quantification of Chx10 mRNA$^+$ cells at E17. Error bars as in Figure 4. Scale bar in **A** is 50 μm.

Chx10 is expressed exclusively in progenitors (Liu et al., 1994) and bipolar cell birth has not commenced (Figure 1B). The number of Chx10$^+$ cells was not different in WT, RBKO, or DKO retina (Figure 6D). Together, these data suggest that, in contrast to the dramatic effect in precursors, RB/p107 loss does not affect the cell cycle in progenitors.

Retinoblastoma in the peripheral DKO retina: Tumor cells express INL determinants

In chimeras, retinoblastoma requires deletion of both *Rb* and *p107* (Robanus-Maandag et al., 1998). Thus, unless *Rb* deletion was required prior to retinogenesis, we expected to observe tumors in our DKO model. Indeed, retinoblastoma was observed as early as P8 in many animals, and larger tumors that filled the vitreous were evident at later stages (Figures 7A–7C, Supplemental Table S2). Retinoblastoma was present in 68% or 60% of P8–P60 DKO animals or eyes, respectively (Supplemental Table S1). Tumors arose from the peripheral retina (Figure 7A), where RB was absent (Figure 2C), and analysis of microdissected material confirmed that tumors contained only the recombined *Rb* null allele (Supplemental Figure S3). These mice represent the first inheritable model of retinoblastoma induced by *Rb* gene inactivation.

We did not observe tumors in RBKO retina, indicating that p107 suppresses retinoblastoma following acute *Rb* loss during retinal development. We also did not detect abnormalities in the $Rb^{+/-};p107^{-/-}$ retina, suggesting that the dysplasia seen in $Rb^{+/-};p107^{-/-}$ mice (Lee et al., 1996) may require *Rb* loss prior to retinogenesis.

To assess tumor origin, emerging P8 and established P30 tumors were assessed for the expression of cell type determinants and other differentiation markers. Nascent P8 tumors contained many dividing cells that expressed both NeuroD and Math3, which are essential for amacrine cell genesis (Inoue et al., 2002), and Hes5, which drives Müller glia differentiation (Hojo et al., 2000) (Figures 7D–7H). In contrast, few death-prone Crx$^+$ photoreceptor, Chx10$^+$ bipolar, or Brn3b$^+$ ganglion precursors were detected (Figures 7I–7N). These cells might the result of mixing of the invading expanding tumor with surrounding nontransformed DKO cells or adjacent WT cells. Indeed, low-magnification views of the P8 tumor shown in Figure 7 suggested that it had pushed the neighboring WT GCL toward the vitreous, and engulfed Crx$^+$ and Chx10$^+$ cells primarily at its base (Figures 7I–7N). These cells are a likely source of the apoptosis detected in microtumors (Figure 7O). Mixing is inevitable since tumors arise from the INL and at a time when there is ectopic division of all precursors. Consistent with the idea that the transformed cells arise from surviving INL precursors, mature P30 tumors consisted solely of dividing cells that expressed NeuroD and Math3 (Figures 7P–7S), as well as other amacrine markers such as Pax6, syntaxin, and calretinin (Figures 7U–7W), and a small but significant fraction of cells expressing Müller markers Hes5, GFAP, and CRALBP (Figures 7T, 7V, and 7X). In contrast, P30 tumors lacked cells expressing photoreceptor, bipolar, or ganglion cell determinants or later stage markers for these cell types and were TUNEL$^-$, supporting the idea that the sporadic presence of these markers at earlier stages was due to contamination (Figures 7Y–7BB and data not shown). Together, the data suggest a model in which retinoblastoma arises from death-resistant INL precursors rather than death-prone ganglion, bipolar, rod, or cone precursors.

Discussion

RB loss perturbs precursor cell cycle exit

Retinal cells traverse three basic developmental stages: expansion of progenitors, differentiation into postmitotic precursors, and terminal differentiation into seven cell types (Figure 1A). Expression studies suggested that RB is absent in embryonic progenitors but present in most postnatal progenitors, and RBKO explants generate more cells than WT explants (Gallie et al., 1999; Jiang et al., 1997; Zhang et al., 2004). However, these analyses did not reveal whether RB controls the rate

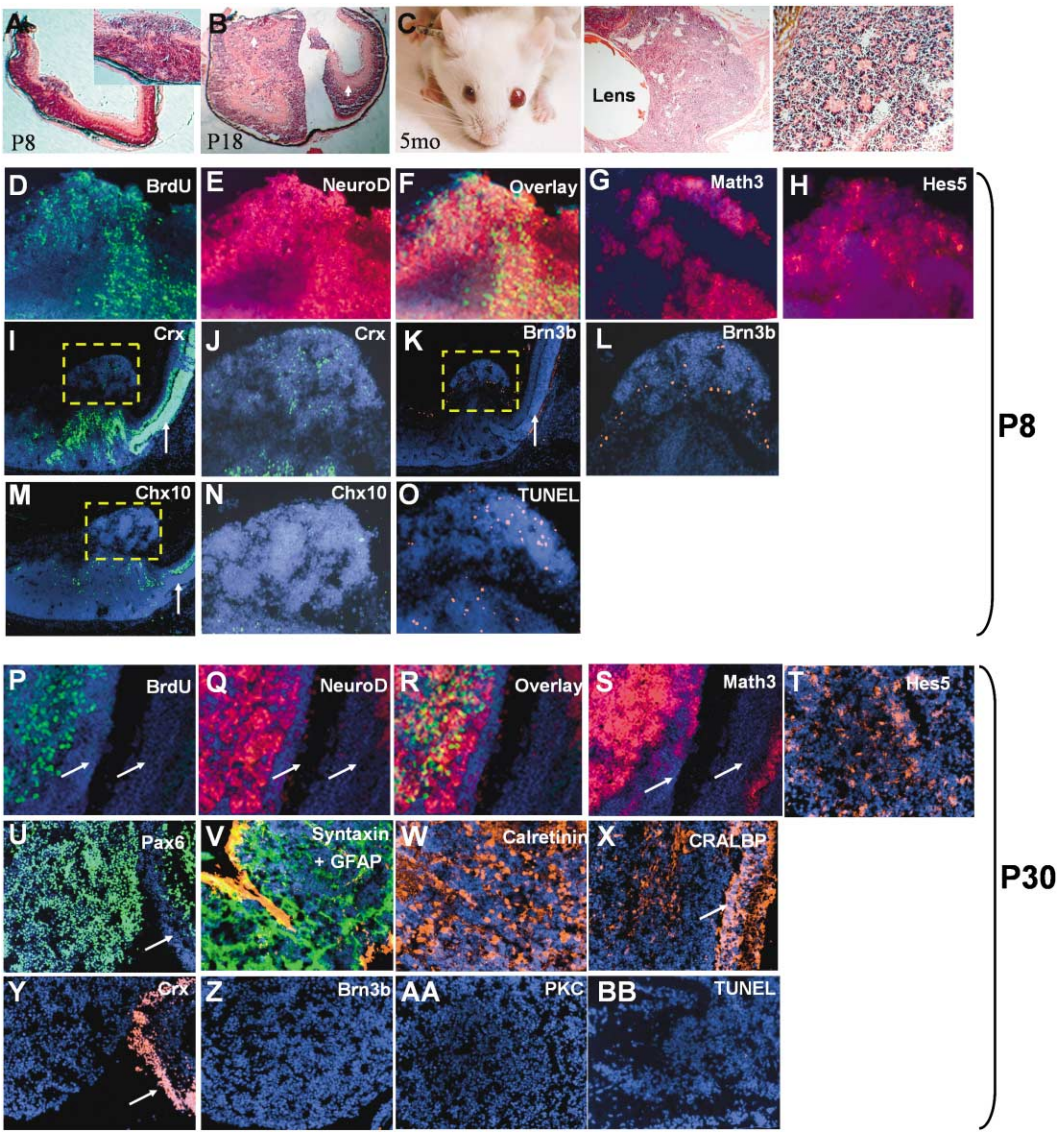

Figure 7. Cells expressing amacrine precursor determinants dominate mouse retinoblastoma

A: Hematoxylin and eosin (H&E)-stained section from *Rb*$^{loxP/loxP}$;*p107*$^{-/-}$;α-*Cre* P8 retinas. Inset shows blow-up of tumor emerging from the INL and invading the vitreous.
B: Larger H&E-stained tumor at P18. Note that tumor staining resembles the normal differentiated inner retina where amacrine cells reside (arrowheads).
C: Five-month-old mouse with tumor that has filled the vitreous causing the eye to protrude. H&E-stained section at far right shows rosettes.
D–O: Emerging P8 tumor stained for nuclei (DAPI, blue) and BrdU (**D** and **F**, green), NeuroD (**E** and **F**, red), Math3 (**G**, red), Hes5 (**H**, red), Crx (**I** and **J**, green), Brn3b (**K** and **L**, red), Chx10 (**M** and **N**, green), or TUNEL (**O**, red). The boxed regions in **L**, **K**, and **M** are shown at higher magnification in **J**, **L**, and **M**.
P–BB, Established P30 tumor stained for nuclei (DAPI, blue) and BrdU (**P** and **R**, green), NeuroD (**Q** and **R**, red), Math3 (**S**, red), Hes5 (**T**, red), Pax6 (**U**, green), syntaxin (**V**, green) plus GFAP (**V**, red), calretinin (**W**, red), CRALBP (**X**, red), Crx (**Y**, red), Brn3b (**Z**, red), PKCα (**AA**, green), or TUNEL (**BB**, red). Some sections include WT retina (arrows) adjacent to the tumor. Note the contrast in BrdU labeling between P30 tumor and WT retina (**P** and **R**). NeuroD, Math3, and Hes5 results are in situ hybridizations. Other data represent immunofluorescence analysis. Section showing Math3 staining at P8 (**G**) is from near the end of the tumor, hence there are fewer total cells than in other panels.

and/or extent of retinal progenitor division and/or cell cycle exit during the birth of one or more precursors, which is critical to understand the origin of retinoblastoma. We present functional evidence that RB or RB/p107 loss has a drastic effect on cell cycle exit in precursors. S and M phase RBKO or DKO cells were identified in ectopic positions, and at times after proliferation normally ends, double labeling confirmed that all seven DKO precursors were specified and divided ectopically, and repeated BrdU injections after P1 labeled numerous RBKO and DKO amacrine cells, which are born prior to P1. Thus, RB or RB/p107 loss does not block precursor specification, but perturbs cell cycle exit in all precursors.

In contrast, RB and p107 do not have major roles in controlling progenitor cell division. The number of normal mitotic progenitors on the ventricular surface was not different in WT, RBKO, or DKO E17 or P0 retina, and the E17 RBKO or DKO

retina contained normal numbers of Chx10$^+$ progenitors. Also, if *Rb* loss impaired the transition of progenitors to precursors, there might be more late-born cells at the expense of early-born cells, but there were many early-born cell types in the RBKO retina.

Collectively, these results indicate that RB or RB/p107 loss has little effect on progenitor cell division or precursor specification, but uncouples cell cycle exit from differentiation. These data favor the precursor over the progenitor as the cell-of-origin of mouse retinoblastoma.

The route to transformation: Bypassing terminal differentiation, not death

Transgenic and chimeric studies (Howes et al., 1994; Robanus-Maandag et al., 1994, 1998) provided indirect evidence for the idea that the retinoblastoma cell-of-origin must overcome a propensity to undergo apoptosis (Figure 1C) (Gallie et al., 1999). However, *p53* mutations, essential for tumorigenesis in transgenic models, are not seen in human retinoblastoma or in mouse retinoblastoma derived from DKO cells (Gallie et al., 1999; Robanus-Maandag et al., 1998). Moreover, *p53* loss does not rescue apoptosis or facilitate tumorigenesis in the RBKO retina (Macpherson et al., 2004). Finally, it has never been resolved whether all ectopically dividing DKO retinal cell types are death-prone.

We have provided a comprehensive analysis of the cell-specific effects of RB/p107 loss in the mammalian retina. Consistent with data from chimeric mice (Robanus-Maandag et al., 1998), considerable apoptosis was detected in the DKO retina. Our results reveal that ganglion, cone, rod, and bipolar cells are deleted while, remarkably, horizontal, amacrine, and Müller glia survive and differentiate. Absent cells were specified, since Brn3b$^+$ ganglion, Crx$^+$ photoreceptor, Trβ2$^+$ cone, and Crx$^+$/Chx10$^+$ bipolar precursor were all present in the developing DKO retina. Their disappearance correlated with increased apoptosis, and double labeling proved that ganglion cells but not amacrine precursors underwent apoptosis. We do not rule out the possibility that some horizontal, amacrine, or Müller precursors die as precursors, or that excess cells produced by ectopic division are later pared back due to lack of trophic support. However, the results show that horizontal, amacrine, and Müller precursors have a much greater tolerance for unscheduled DNA synthesis than rod, cone, ganglion, and bipolar cell precursors, and can form a laminated retina.

Previously, it was suggested that *Rb* loss might generate precursors that have infinite proliferative capacity, but are death-prone (Figure 1C) (Gallie et al., 1999). Our data support another model (Figure 1D). Three insights are critical. (1) A subset of INL cell precursors survive RB or RB/p107 loss, making them attractive candidates for the tumor cell-of-origin. (2) Surviving RBKO or DKO precursors divide ectopically, but for a finite period, and exit the cell cycle by P30. Thus, inactivating RB does not create precursors with infinite proliferative capacity. Amacrine cells formed a synaptic layer and Müller glia extended long processes and also underwent reactive gliosis, indicating terminal differentiation. Thus, cells that tolerate ectopic division escape tumorigenesis not through death, but by growth arrest associated with terminal differentiation. By extension, recurrent genetic lesions in human retinoblastoma other than *Rb* loss (Chen et al., 2001, 2002) might not be required to overcome apoptosis, but to adjust the balance between proliferation and terminal differentiation (Figure 1D). (3) Emerging and mature tumors are dominated by dividing cells expressing NeuroD and Math3, essential determinants of amacrine cell genesis (Inoue et al., 2002). Thus, consistent with the differentiation model (Figure 1D), tumors arise from a naturally death-resistant precursor. Mature tumors were devoid of precursor or mature rod, cone, bipolar, or ganglion cells, and emerging tumors contained only sporadic cells with these markers, suggestive of mixing with nontransformed DKO or neighboring WT cells. Such mixing is expected, since tumors arise from the INL at a time when there is ectopic division of all precursors. Tumors also contained Müller (Hes5$^+$) precursors, but the proportion of these cells was reduced in mature versus small emerging P8 tumors. All DKO Müller cells divide at P8 and exit the cell cycle by P30; thus, the simplest interpretation is that emerging P8 tumors contain both transformed amacrine precursors and ectopically dividing nontransformed Müller precursors, and mature tumors contain dividing amacrine and quiescent Müller cells. The idea that amacrine precursors are more tumor-prone than Müller precursors is supported by the observation that expressing E1A in progenitors at P0, the end of amacrine cell genesis and near the start of Müller cell genesis, does not induce tumorigenesis (Zhang et al., 2004). Alternative interpretations of our findings include the possibility that both amacrine and Müller precursors are transformed, or that tumors arise from a precursor capable of generating both amacrine neurons and Müller glia. Irrespective, the major implication is that tumors derive from a naturally death-resistant INL precursor, not one of the four death-prone precursors (Figure 1D).

We cannot formally exclude the possibility that a death-prone rod, cone, bipolar, or ganglion precursor acquires a mutation that simultaneously overrides apoptosis and converts it to an INL precursor. If correct, this model still underscores the idea that tumors exploit the natural ability of some INL precursors to resist apoptosis. We do not favor this model, because logic dictates that the probability of sustaining a transforming mutation is considerably higher in abundant multiplying INL precursors than in photoreceptor, bipolar, or ganglion cell precursors, which are deleted soon after they are generated.

A third model of retinoblastoma proposed that *Rb* loss might generate cells that divide slowly, and additional mutations accelerate division (Zacksenhaus, 2003). Our data suggest that *Rb* or *Rb/p107* loss affects the *extent* of proliferation, but further work is required to establish whether the rate is different in ectopically dividing nontransformed versus transformed precursors. We emphasize the unexpected finding that even DKO cells eventually exit the cell cycle, lending support to the idea that the critical barrier to transformation is terminal differentiation, rather than the rate of proliferation.

Which factors allow RBKO or DKO retinal cells to exit the cell cycle? One possibility is the remaining member of the RB family, p130, which is upregulated during the terminal differentiation of many cell types (Mulligan and Jacks, 1998). Indeed, the Rb$^{-/-}$;p130$^{-/-}$ mouse retina also develops retinoblastoma (Macpherson et al., 2004). Other cell cycle-inhibitory molecules, such as p21^{Cip1} or p27^{Kip1}, can block division in the absence of RB (reviewed in (Herwig and Strauss, 1997)). Intriguingly, many of the chromosomal regions altered in human retinoblastoma include genes involved in cell cycle regulation (Chen et al., 2001). Finally, Harris recently argued that cancer should be viewed "as a disease of cell differentiation rather than multiplication" (Harris,

2004); thus, cell cycle regulators may lie downstream of signals that trigger terminal differentiation in DKO cells.

Effects of RB loss in different models

Our data are the first to describe the cell-specific effects of loss of both *Rb* and *p107* on retinal development. The effects of *Rb* loss alone have been analyzed recently by Zhang et al. (2004), using a combination of explant and Cre-lox models. In the explant studies, it was impossible to study ganglion cell development because these cells die even in WT explants, but in agreement with our finding that *Rb* loss compromises the survival of many rods and most bipolar cells, E13 $Rb^{-/-}$ explants grown for 12 days in vitro (DIV) generated all mature retinal cell types except rods, while E18.5 retinal explants grown from $Rb^{-/-}$ embryos with a normal placenta lacked most rods and half the bipolar cells (Zhang et al., 2004). Surprisingly, there was no increased apoptosis in $Rb^{-/-}$ explants grown from E13 retina. This finding contrasts with our data, an independent analysis of RBKO retina in vivo (Macpherson et al., 2004), and chimeric studies in which $Rb^{-/-}$ cells were underrepresented in the retina (Robanus-Maandag et al., 1994), suggesting distinct effects of *Rb* loss in vitro and in vivo. Zhang et al. also developed a Cre-lox model based on a transgene that is active at E11 and expresses in patches of ~500 cells. Consistent with our results, patches of rod-negative ONL were observed, although data on apoptosis or the status of bipolar or ganglion cells were not reported. Inactivation of *Rb* in isolated P0 progenitors using a Cre retrovirus does not affect the composition of resulting clones (Zhang et al., 2004). The survival of all sporadic $Rb^{-/-}$ cells could mean that cell death in the α-Cre model (this work) is non-cell-autonomous, or that *Rb* inactivation at P0 is less detrimental than at embryonic stages. Chimeric data suggest that loss of $Rb^{-/-}$ retinal cells is a cell-autonomous effect, although it is conceivable that the fraction of WT cells was too low to rescue $Rb^{-/-}$ cells. If sporadic $Rb^{-/-}$ cells are not deleted, this would strengthen the idea that retinoblastoma arises from precursors that are intrinsically death-resistant (Figure 1D).

Zhang et al. noted that surviving rods in *Rb*-deficient retina exhibited abnormal structure and attributed this to a role for RB in rod differentiation. Such a function cannot be ruled out, but it is difficult to interpret whether the effect is direct, or an indirect result of perturbing cell cycle exit, which we show affects precursors. Cre-mediated inactivation of *Rb* in postmitotic photoreceptor precursors has no reported effect on terminal differentiation, even in the absence of *p107* and *p53* (Vooijs et al., 2002).

Comparing mouse and human retinoblastoma

Unlike the human disease, mouse retinoblastoma requires inactivation of both *Rb* and *p107* (Robanus-Maandag et al., 1998 and this work). Thus, it is important to consider how our findings relate to the human disease. Many markers of mature retinal cell types have been detected in human retinoblastoma (Nork et al., 1995). We envisage three explanations as to why the tumors described here are more specific for INL markers. (1) The mouse model may not mimic human retinoblastoma. However, the fundamental role of RB in regulating cell cycle exit in every type of mouse retinal precursor (this work) suggests that this function will be conserved in humans. (2) Both human and mouse retinoblastoma may arise from INL precursors, but accumulated mutations might drive transdifferentiation of late-stage tumor cells. Most marker analyses utilize large, mature tumors isolated months or years after the cancer initiated. Notably, nascent human retinoblastoma has been observed arising solely from the INL (Gallie et al., 1999). (3) It is possible that sporadic $Rb^{-/-}$ precursors are death-resistant, in which case, the fraction of tumors expressing different markers would reflect the relative population of each corresponding cell type. Indeed, a large percentage of retinoblastoma tumors express photoreceptor markers, the most abundant retinal cell type (Nork et al., 1995).

Bern's group provided the first p53-independent mouse model of retinoblastoma (Robanus-Maandag et al., 1998). However, in the chimeric mice, there is variable contribution of mutant cells, the survival rate of embryos is erratic, the disease is not inheritable, and the approach is challenging. The inheritable models described here and elsewhere (Macpherson et al., 2004) will simplify analysis of the cell-of-origin of retinoblastoma, elucidation of the genetic events linked to disease progression, and comparison of the molecular features in mouse versus human retinoblastoma, and provide valuable insight into the effectiveness of existing and new treatments. Pathways that control the balance between division and terminal differentiation, or death and survival, in $Rb^{-/-}$ precursors present excellent avenues for the development of novel therapies.

Relevance to other cancers

Resistance to apoptosis is a hallmark of tumor cells and is typically acquired through mutation (Hanahan and Weinberg, 2000). Our data suggest that some tumors need not acquire this characteristic if they arise from the appropriate cell type. Intrinsic death resistance is an ideal feature of a cancer cell-of-origin, and may help explain why pediatric tumors reach malignancy in fewer steps than adult cancers.

The importance of understanding the properties of a cancer cell-of-origin is underscored by the distinct effects of oncogenes in different cell types. For example, SV40 large T antigen has no effect on some neurons, induces apoptosis in others, and transforms only a subset (Al-Ubaidi et al., 1992a, 1992b; Baetscher et al., 1991; Efrat et al., 1988). It may be possible to exploit the strengths of resistant cells, or attack the weaknesses of cancer-prone cells to intervene very early in tumorigenesis. Unfortunately, we know little about any cancer cell-of-origin, because the initiating mutation and cell-of-origin are poorly defined in most cases. Retinoblastoma is an important exception, since the initiating mutation is always *Rb* inactivation, and our data pinpoint precursors as the tumor-prone population. Thus, just as retinoblastoma provided the classic two-hit hypothesis (Knudson, 1971) and yielded the first tumor suppressor gene (Friend et al., 1986), it may also provide critical insight into the unique properties of a cancer cell-of-origin. These advances may be of broad utility, since RB is part of a pathway that is defective in most human tumors.

Experimental procedures

Mouse strains and genotyping

Mice were treated according to national guidelines. α-cre mice, $p107^{-/-}$ mice and $Rb^{loxP/loxP}$ mice were maintained on a mixed (NMRI × C57/Bl × FVB/N) background. Mice of different genotypes were compared within the same litter and across a minimum of three litters. Genotyping was as described (LeCouter et al., 1998; Marino et al., 2000; Robanus-Maandag et al., 1998). The bicistronic α-Cre-IRES-GFP cassette allows visual detection of transgene inheritance at birth (Marquardt et al., 2001). Rosa26R mice were from Jackson Laboratories.

Histology, immunofluorescence, and in situ hybridization

Eyeballs were fixed in 4% paraformaldehyde for 1 hr at 4°C, embedded in OCT (TissueTek 4583), frozen on dry ice and cut into 12 μm sections on Superfrost slides, and stained with hematoxylin and eosin. BrdU (100 μg/g of body weight) was injected intraperitoneally 2 hr before sacrifice. For antibodies see Supplemental Table S1 at http://www.cancercell.org/cgi/content/full/5/6/539/DC1. For double labeling of BrdU and cell specific markers, sections were first stained for the cell marker, refixed with 4% paraformaldehyde for 5 min, then washed and treated with 1N HCl and stained for BrdU. TUNEL was as described (Ferguson et al., 2002). Nuclei were counterstained with 4,6-diamidino-2-phenyindole (DAPI; Sigma). In situ hybridization was as described (Schaeren-Wiemers and Gerfin-Moser, 1993) with some modifications: Digoxigenin-labeled probes were visualized using Fast Red (Roche), after which slides were washed in PBS and processed further for immunocytochemistry. Labeled cells were visualized using a Zeiss Axioplan-2 microscope with Plan Neofluar objectives and images captured with a Zeiss AxionCam camera. For double-labeled samples, confocal images were obtained with a Zeiss LSM 5.0 laser scanning microscope.

Measurements

The retina was separated into bins by dividing the ventricular edge of the retina into equal parts and extending a line to the vitreal edge (Figure 2A). Bin1 contains only cells that expressed α-Cre as progenitors, as judged by absence of RB protein. For cell counts or thickness measurement, we used a region 0–100 μm peripheral to the boundary separating Bin1 and Bin2 (Figure 2A). Measurements were performed with Axiovison software. Quantification of S phase, M phase, and apoptotic cells used horizontal sections that included the optic nerve. Quantification of differentiated cell types used horizontal sections at equal distances from the optic nerve. At least three sections per eye and three eyes from different litters were counted. Statistic analysis used the Student's t test. p values are based on two-sided hypothesis testing.

Laser capture microscopy

Tumor cells were dissected from 10 μm H&E sections using the PALM microlaser system and catapulted into the buffer (1 mM EDTA; 20 mM Tris [pH 8]) containing 2 mg/ml Proteinase K. Cells were incubated at 55°C overnight in 10 μl of catapult buffer followed by heat inactivation of proteinase K at 99°C for 10 min. 5 μl of the buffer was used for each PCR.

Acknowledgments

We thank A. Berns, P. Gruss, and M. Rudnicki for mice, P.A. Hargrave, C.Y. Gregory-Evans, C.M. Craft, X. Zhu, R. McInnes, R.L. Chow, and J. Saari for antibodies, R. Kageyama for probes, A. Balmain, B. Gallie, V. Wallace, J. Woodgett, J. Wrana, and E. Zacksenhaus for comments, and D. Macpherson and T. Jacks for sharing unpublished results. This work was supported by a grant from the Canadian Institute for Health Research to R.B. D.C. was supported in part by the Helen Keller Foundation and Fight for Sight.

Received: December 20, 2003
Revised: March 26, 2004
Accepted: May 18, 2004
Published: June 14, 2004

References

Al-Ubaidi, M.R., Font, R.L., Quiambao, A.B., Keener, M.J., Liou, G.I., Overbeek, P.A., and Baehr, W. (1992a). Bilateral retinal and brain tumors in transgenic mice expressing simian virus 40 large T antigen under control of the human interphotoreceptor retinoid-binding protein promoter. J. Cell Biol. *119*, 1681–1687.

Al-Ubaidi, M.R., Hollyfield, J.G., Overbeek, P.A., and Baehr, W. (1992b). Photoreceptor degeneration induced by the expression of simian virus 40 large tumor antigen in the retina of transgenic mice. Proc. Natl. Acad. Sci. USA *89*, 1194–1198.

Baetscher, M., Schmidt, E., Shimizu, A., Leder, P., and Fishman, M.C. (1991). SV40 T antigen transforms calcitonin cells of the thyroid but not CGRP-containing neurons in transgenic mice. Oncogene *6*, 1133–1138.

Bibb, L.C., Holt, J.K., Tarttelin, E.E., Hodges, M.D., Gregory-Evans, K., Rutherford, A., Lucas, R.J., Sowden, J.C., and Gregory-Evans, C.Y. (2001). Temporal and spatial expression patterns of the CRX transcription factor and its downstream targets. Critical differences during human and mouse eye development. Hum. Mol. Genet. *10*, 1571–1579.

Burmeister, M., Novak, J., Liang, M.Y., Basu, S., Ploder, L., Hawes, N.L., Vidgen, D., Hoover, F., Goldman, D., Kalnins, V.I., et al. (1996). Ocular retardation mouse caused by Chx10 homeobox null allele: Impaired retinal progenitor proliferation and bipolar cell differentiation. Nat. Genet. *12*, 376–384.

Chen, S., Wang, Q.L., Nie, Z., Sun, H., Lennon, G., Copeland, N.G., Gilbert, D.J., Jenkins, N.A., and Zack, D.J. (1997). Crx, a novel Otx-like paired-homeodomain protein, binds to and transactivates photoreceptor cell-specific genes. Neuron *19*, 1017–1030.

Chen, D., Gallie, B.L., and Squire, J.A. (2001). Minimal regions of chromosomal imbalance in retinoblastoma detected by comparative genomic hybridization. Cancer Genet. Cytogenet. *129*, 57–63.

Chen, D., Pajovic, S., Duckett, A., Brown, V.D., Squire, J.A., and Gallie, B.L. (2002). Genomic amplification in retinoblastoma narrowed to 0.6 megabase on chromosome 6p containing a kinesin-like gene, RBKIN. Cancer Res. *62*, 967–971.

Clarke, A.R., Maandag, E.R., Van Roon, M., Van der Lugt, N.M.T., Van der Valk, M., Hooper, M.L., Berns, A., and Te Riele, H. (1992). Requirement for a functional Rb-1 gene in murine development. Nature *359*, 328–330.

Dyer, M.A., Livesey, F.J., Cepko, C.L., and Oliver, G. (2003). Prox1 function controls progenitor cell proliferation and horizontal cell genesis in the mammalian retina. Nat. Genet. *34*, 53–58.

Efrat, S., Teitelman, G., Anwar, M., Ruggiero, D., and Hanahan, D. (1988). Glucagon gene regulatory region directs oncoprotein expression to neurons and pancreatic alpha cells. Neuron *1*, 605–613.

Erkman, L., McEvilly, R.J., Luo, L., Ryan, A.K., Hooshmand, F., O'Connell, S.M., Keithley, E.M., Rapaport, D.H., Ryan, A.F., and Rosenfeld, M.G. (1996). Role of transcription factors Brn-3.1 and Brn-3.2 in auditory and visual system development. Nature *381*, 603–606.

Ferguson, K.L., Vanderluit, J.L., Hebert, J.M., McIntosh, W.C., Tibbo, E., MacLaurin, J.G., Park, D.S., Wallace, V.A., Vooijs, M., McConnell, S.K., and Slack, R.S. (2002). Telencephalon-specific Rb knockouts reveal enhanced neurogenesis, survival and abnormal cortical development. EMBO J. *21*, 3337–3346.

Freund, C.L., Gregory-Evans, C.Y., Furukawa, T., Papaioannou, M., Looser, J., Ploder, L., Bellingham, J., Ng, D., Herbrick, J.A., Duncan, A., et al. (1997). Cone-rod dystrophy due to mutations in a novel photoreceptor-specific homeobox gene (CRX) essential for maintenance of the photoreceptor. Cell *91*, 543–553.

Friend, S.H., Bernards, R., Rogelj, S., Weinberg, R.A., Rapaport, J.M., Albert, D.M., and Dryja, T.P. (1986). A human DNA segment with properties of the gene that predisposes to retinoblastoma and osteosarcoma. Nature *323*, 643–646.

Furukawa, T., Morrow, E.M., and Cepko, C.L. (1997). Crx, a novel otx-like homeobox gene, shows photoreceptor-specific expression and regulates photoreceptor differentiation. Cell *91*, 531–541.

Gallie, B.L., Campbell, C., Devlin, H., Duckett, A., and Squire, J.A. (1999). Developmental basis of retinal-specific induction of cancer by RB mutation. Cancer Res. *59*, 1731s–1735s.

Gan, L., Xiang, M., Zhou, L., Wagner, D.S., Klein, W.H., and Nathans, J. (1996). POU domain factor Brn-3b is required for the development of a large set of retinal ganglion cells. Proc. Natl. Acad. Sci. USA *93*, 3920–3925.

Hanahan, D., and Weinberg, R.A. (2000). The hallmarks of cancer. Cell *100*, 57–70.

Harris, H. (2004). Tumour suppression: putting on the brakes. Nature *427*, 201.

Herwig, S., and Strauss, M. (1997). The retinoblastoma protein: A master

regulator of cell cycle, differentiation and apoptosis. Eur. J. Biochem. *246*, 581–601.

Hojo, M., Ohtsuka, T., Hashimoto, N., Gradwohl, G., Guillemot, F., and Kageyama, R. (2000). Glial cell fate specification modulated by the bHLH gene Hes5 in mouse retina. Development *127*, 2515–2522.

Howes, K.A., Ransom, N., Papermaster, D.S., Lasudry, J.G., Albert, D.M., and Windle, J.J. (1994). Apoptosis or retinoblastoma: alternative fates of photoreceptors expressing the HPV-16 E7 gene in the presence or absence of p53. Genes Dev. *8*, 1300–1310.

Inoue, T., Hojo, M., Bessho, Y., Tano, Y., Lee, J.E., and Kageyama, R. (2002). Math3 and NeuroD regulate amacrine cell fate specification in the retina. Development *129*, 831–842.

Jacks, T., Fazeli, A., Schmitt, E.M., Bronson, R.T., Goodell, M.A., and Weinberg, R.A. (1992). Effects of an *Rb* mutation in the mouse. Nature *359*, 295–300.

Jiang, Z., Zacksenhaus, E., Gallie, B.L., and Phillips, R.A. (1997). The retinoblastoma gene family is differentially expressed during embryogenesis. Oncogene *14*, 1789–1797.

Knudson, A.G.J. (1971). Mutation and cancer: statistical study of retinoblastoma. Proc. Natl. Acad. Sci. USA *68*, 820–823.

LeCouter, J.E., Kablar, B., Hardy, W.R., Ying, C., Megeney, L.A., May, L.L., and Rudnicki, M.A. (1998). Strain-dependent myeloid hyperplasia, growth deficiency, and accelerated cell cycle in mice lacking the Rb-related p107 gene. Mol. Cell. Biol. *18*, 7455–7465.

Lee, E.Y.H.P., Chang, C.Y., Hu, N., Wang, Y.C.J., Lai, C.C., Herrup, K., Lee, W.H., and Bradley, A. (1992). Mice deficient for Rb are nonviable and show defects in neurogenesis and haematopoiesis. Nature *359*, 288–294.

Lee, M.H., Williams, B.O., Mulligan, G., Mukai, S., Bronson, R.T., Dyson, N., Harlow, E., and Jacks, T. (1996). Targeted disruption of p107: Functional overlap between p107 and Rb. Genes Dev. *10*, 1621–1632.

Liu, I.S.C., Chen, J., Ploder, L., Vidgen, D., van der Kooy, D., Kalnins, V.I., and McInnes, R.R. (1994). Developmental expression of a novel murine homeobox gene (Chx10): Evidence for roles in determination of the neuroretina and inner nuclear layer. Neuron *13*, 377–393.

Macpherson, D., Sage, J., Kim, T., Ho, D., and Jacks, T. (2004). Cell-type specific effects of Rb deletion in the murine retina. Genes Dev., in press

Marino, S., Vooijs, M., van Der Gulden, H., Jonkers, J., and Berns, A. (2000). Induction of medulloblastomas in p53-null mutant mice by somatic inactivation of Rb in the external granular layer cells of the cerebellum. Genes Dev. *14*, 994–1004.

Marino, S., Hoogervoorst, D., Brandner, S., and Berns, A. (2003). Rb and p107 are required for normal cerebellar development and granule cell survival but not for Purkinje cell persistence. Development *130*, 3359–3368.

Marquardt, T., Ashery-Padan, R., Andrejewski, N., Scardigli, R., Guillemot, F., and Gruss, P. (2001). Pax6 is required for the multipotent state of retinal progenitor cells. Cell *105*, 43–55.

Mulligan, G., and Jacks, T. (1998). The retinoblastoma gene family: Cousins with overlapping interests. Trends Genet. *14*, 223–229.

Ng, L., Hurley, J.B., Dierks, B., Srinivas, M., Salto, C., Vennstrom, B., Reh, T.A., and Forrest, D. (2001). A thyroid hormone receptor that is required for the development of green cone photoreceptors. Nat. Genet. *27*, 94–98.

Nork, T.M., Schwartz, T.L., Doshi, H.M., and Millecchia, L.L. (1995). Retinoblastoma. Cell of origin. Arch. Ophthalmol. *113*, 791–802.

Rakic, S., and Zecevic, N. (2000). Programmed cell death in the developing human telencephalon. Eur. J. Neurosci. *12*, 2721–2734.

Robanus-Maandag, E.C., Van der Valk, M., Vlaar, M., Feltkamp, C., O'Brien, J., Van Roon, M., Van der Lugt, N., Berns, A., and Te Reile, H. (1994). Developmental rescue of an embryonic-lethal mutation in the retinoblastoma gene in chimeric mice. EMBO J. *13*, 4260–4268.

Robanus-Maandag, E., Dekker, M., van der Valk, M., Carrozza, M.L., Jeanny, J.C., Dannenberg, J.H., Berns, A., and te Riele, H. (1998). p107 is a suppressor of retinoblastoma development in pRb-deficient mice. Genes Dev. *12*, 1599–1609.

Saavedra, H.I., Wu, L., de Bruin, A., Timmers, C., Rosol, T.J., Weinstein, M., Robinson, M.L., and Leone, G. (2002). Specificity of E2F1, E2F2, and E2F3 in mediating phenotypes induced by loss of Rb. Cell Growth Differ. *13*, 215–225.

Schaeren-Wiemers, N., and Gerfin-Moser, A. (1993). A single protocol to detect transcripts of various types and expression levels in neural tissue and cultured cells: in situ hybridization using digoxigenin-labelled cRNA probes. Histochemistry *100*, 431–440.

Usukura, J., Khoo, W., Abe, T., Breitman, M.L., and Shinohara, T. (1994). Cone cells fail to develop normally in transgenic mice showing ablation of rod photoreceptor cells. Cell Tissue Res. *275*, 79–90.

Vooijs, M., Te Riele, H., Van Der Valk, M., and Berns, A. (2002). Tumor formation in mice with somatic inactivation of the retinoblastoma gene in interphotoreceptor retinol binding protein-expressing cells. Oncogene *21*, 4635–4645.

Watanabe, M., Hitomi, M., van der Wee, K., Rothenberg, F., Fisher, S.A., Zucker, R., Svoboda, K.K., Goldsmith, E.C., Heiskanen, K.M., and Nieminen, A.L. (2002). The pros and cons of apoptosis assays for use in the study of cells, tissues, and organs. Microsc. Microanal. *8*, 375–391.

Wu, L., De Bruin, A., Saavedra, H.I., Starovic, M., Trimboli, A., Yang, Y., Opavska, J., Wilson, P., Thompson, J.C., Ostrowski, M.C., et al. (2003). Extra-embryonic function of Rb is essential for embryonic development and viability. Nature *421*, 942–947.

Xiang, M., Zhou, L., Peng, Y.W., Eddy, R.L., Shows, T.B., and Nathans, J. (1993). Brn-3b: A POU domain gene expressed in a subset of retinal ganglion cells. Neuron *11*, 689–701.

Young, R.W. (1985). Cell proliferation during postnatal development of the retina in the mouse. Brain Res. *353*, 229–239.

Zacksenhaus, E. (2003). Alternative reading frame supports an alternative model for retinoblastoma. Cell Cycle *2*, 27–30.

Zhang, J., Gray, J., Wu, L., Leone, G., Rowan, S., Cepko, C.L., Zhu, X., Craft, C.M., and Dyer, M.A. (2004). Rb regulates proliferation and rod photoreceptor development in the mouse retina. Nat. Genet. *36*, 351–360.